Six-Dimensional Energy-Switching Potential Energy Surface for HeHCN

Wazir-ul H. Ansari[†] and António J. C. Varandas*

Departamento de Química, Universidade de Coimbra 3004-535 Coimbra, Portugal

Received: May 14, 2002; In Final Form: August 2, 2002

A single-valued six-dimensional (6D) potential energy surface is determined for HeHCN by using the energy switching (ES) method, which utilizes a global double many-body expansion (DMBE) as well as a Legendre polynomial expansion for different energy regimes. The ES potential has a linear van der Waals well of 29.5 cm^{-1} which is about 4 cm^{-1} lower than that reported by Drucker et al. [*J. Phys. Chem.* **1995**, *99*, 2646] but agrees with one obtained by Atkins and Hutson [*J. Chem. Phys.* **1996**, *105*, 440]. The effect of stretch of CN as well as CH bonds has also been investigated. With stretch, both the DMBE and ES schemes yield slightly deeper wells and steeper repulsion walls in the high energy region. Microwave transitions calculated at 15.9 and 31.3 GHz agree well with experiment and may be assigned to $J = 1 \leftarrow 0$ and $J = 2 \leftarrow 1$, respectively. This frequency is found to decrease with stretch. Finally, this ES potential energy surface has been compared with that of ArHCN reported by one of us [*Chem. Phys. Lett.* **1998**, *297*, 458]. Here, the question of transferability of the parameter which scales the Hatree-Fock energy in the rare gas-X (X = H, C, and N) interaction from ArHCN to HeHCN has also been investigated. The transferability seems to work as it nicely brings out the position of the potential well and the rovibrational levels. The microwave transition, from the ground state ($j = 0$, $L = 0$, $J = 0$) to state (1, 0, 1), found at 98.61 GHz in HeHCN can be compared with one found at about 162.48 GHz in ArHCN, in close agreement with experiment.

1. Introduction

During the last two decades, there has been increased interest in the study of intermolecular interactions of rare gas(Rg)−HCN van der Waals complexes.[1−15] Monomers and dimers were investigated both experimentally and theoretically.[3,4,9,16−23] An ab initio CEPA-I and MP4 potential energy surface for ArHCN was reported by Clary et al.[2] and Tao et al.,[22] respectively. A host of workers[17,18,21,24,25] experimentally investigated this van der Waals complex, although arriving at no general consensus on the form of its potential energy surface.[22] Gutowsky et al.,[3] while investigating experimentally the microwave rotational transitions of Ne−HCN dimer, have also presented a molecular-mechanics-for-clusters (MMC) potential energy surface for Rg−HCN dimers with He, Ne, Ar, and Kr as rare gas giving stabilities of 21, 37, 85, and 108 cm^{-1}, respectively. Their results also show a quasilinear equilibrium geometry for both He−HCN and Ne−HCN dimers.

The first ab initio potential energy surface for the title van der Waals molecule, good enough to reproduce experimental data on high-resolution ground-state spectroscopy, has been reported a few years ago by Drucker et al.[4] They calculated rovibrational energies and wave functions at the MP4 level using a large basis set containing bond functions. Their function has a well of 25 cm^{-1} at the center of mass separation $R = 4.27$ Å, with a global minimum occurring at the collinear configuration He···HCN, and the minimum energy rising monotonically with large angular-radial coupling, as the HCN orientation angle θ increases from 0 to 2π. Drucker et al.[4] have also reported high-resolution spectroscopy of the bound states of HeHCN. Ground-state $J = 1 \leftarrow 0$ and $J = 2 \leftarrow 1$ transitions were measured at 15 893.6108 and 31 325.2443 MHz, respectively. Their rovibrational energies calculated from an intermolecular Legendre-type potential energy surface agree to within 10% with observed values of mm wave/microwave transition energies.

This work was followed by Atkins and Hutson,[5] who obtained two potential energy surfaces (1E8 and 2E8) for the title system by least-squares fitting to data from high-resolution microwave and millimeter-wave spectroscopy of Drucker et al.[4] The global minimum of 1E8 is at a linear configuration He···HCN with a significantly deeper well of depth 29.47 cm^{-1}, whereas 2E8 has a slightly nonlinear well of 29.36 cm^{-1}. Using the potential energy surfaces, they predict new spectral lines which yet require confirmation.

More recently, Toczylowski et al.[15] reported two-dimensional potential energy surface for Rg−HCN, with Rg = He, Ne, Ar, and Kr, using the CCSD(T) approach and the augmented correlation consistent polarized basis sets with an additional set of bond functions, with a linear well of 29.9 cm^{-1} at $R = 4.22$ Å and a local bent minimum of depth 22.07 cm^{-1} at $R = 3.59$ Å. They also predict bound-state spectral lines that are yet to be confirmed.

The Taylor series or polynomial expanded potential energy functions may accurately reproduce the available vibrational−rotational data, because they are designed to be valid in the vicinity of the potential well to which the fitted data belongs. However, they may not be good enough for our understanding of the dynamics of van der Waals molecular complexes if one looks at the bond-breaking/formation of the chemically stable molecule. For this, one requires a fully dimensional potential energy surface which describes any product channel (including the van der Waals one). The HeHCN potential energy functions of Atkins and Hutson[5] assume the form of a single-channel atom-pseudo-diatom Legendre expansion, with the radial co-

* To whom correspondence should be addressed. E-mail: varandas@qtvs1.qui.uc.pt.

[†] On leave from Department of Physics, LN Mithila University, Darbhanga-846004, India.

10.1021/jp021209x CCC: $22.00
Published on Web 09/11/2002

efficients being in turn written as a Legendre analysis. They also include some empirical elements, which make them reproduce accurately the available rovibrational data. For this work, we have chosen their form 1E8, because this is somewhat simpler and both are expected to lead to very similar results. Of course, we could have equally employed the form 2E8, but this was unavailable to us. The reader should consult the original paper for further details.

A global double many-body expansion (DMBE)[26−28] potential energy surface for ArHCN was presented by one of us[7] for investigating the dynamics of recombination/dissociation of HCN, with the observation that the precise form of the attractive well is relatively unimportant in scattering dynamics and that it is rather the inner repulsive wall that could play a very important role in the dynamics of the system. So, in view of these and similar observations made by Bruehl et al.[29] and Hippler et al.,[30] the global DMBE potential energy surface, which employs the realistic extended Hartree−Fock approximate correlation energy[26,31,32] (EHFACE2U) model, should provide a reliable representation of the potential energy both in the repulsive wall and long-range regions.

The DMBE potential energy surface for ArHCN was found good enough for a detailed dynamics study of the dissociation reaction Ar + HCN → Ar + H + CN.[7] The calculated thermal rate constant was found to be in good agreement with experiment. As the DMBE surface was not found as much good for the bound states of the system, a global ES potential function was then considered by the authors.[7] This global ES potential energy surface[8] has been used to investigate the spectra of van der Waals modes for the ArHCN molecule. Such a surface combines the global DMBE form with a Legendre-type expansion (or a form similar to one used by Tao et al.[22] or other related form, if one so wishes) for the system. This then appears to have a promise of reproducing both the kinetics and rovibrational spectroscopy.

The 6D DMBE surface, or the ES one which entails it, can also be used to investigate an important aspect of molecular structure, associated with bond stretching, as it may be related to the features of the inner repulsive wall of the potential energy surface. The importance of proper representation of the attractive part of the potential surface cannot be overemphasized for the bound states.

While investigating Rg−HCN van der Waals systems, we revisited our work on Ar−HCN[8] and found that a slightly different repulsive function could represent its potential better (see below). Moreover, many-body expanded functions apart from describing correct dissociative behavior have the advantage of providing a data bank[33] of potentials of all fragments needed to build up a polyatomic potential and can be used as a prototype potential.

In view of the above, therefore, we report, in this work, a global 6D energy-switching potential energy surface for HeHCN, along with our results of its application to study the effect of bond stretching on one hand and the microwave transitions of HeHCN on the other, using a slightly different repulsive function than the one we reported for ArHCN and some empirical elements as used by Atkins and Hutson,[5] deferring report of our results on ArHCN. The structure of this paper is as follows. In section 2, we review the methodology. Sections 3 and 4 contain the discussion of results and the concluding remarks, respectively.

2. Methodology

2.1. DMBE Potential Energy Surface. As the ES potential energy surface is constructed from the DMBE and Legendre's expanded functions, we first briefly describe the DMBE methodology, the details of which may be found elsewhere.[26−28,34] Accordingly, the four-body 6D potential for HeHCN may be written as a sum of a realistic DMBE potential energy surface for HCN and relevant two-body potentials involving He atom, with the three-body and four-body terms involving He atom ignored, as a first approximation

$$V(\mathbf{R}) = V_{\mathrm{HCN}}(R_{\mathrm{CN}}, R_{\mathrm{CH}}, R_{\mathrm{NH}}) + \sum_{\beta=\mathrm{C,H,N}} V_{\mathrm{He}\beta}(R_{\mathrm{He}\beta}) \quad (1)$$

where **R** is a collective variable that denotes the six internuclear distances of the system, V_{HCN} is the three-body HCN potential,[35] and the terms under summation sign represent the realistic Hartree−Fock approximate correlation energy (denoted EHFACE2U[26,31,32]) and may, under DMBE scheme be written for He interactions as follows:

$$V_{\mathrm{He}\beta} = \lambda_{\mathrm{He}\beta} V_{\mathrm{HF}}(R) + V_{\mathrm{dc}}(R) \quad (2)$$

where $\lambda_{\mathrm{He}\beta}$ is a scaling parameter fitted to obtain a satisfactory van der Waals potential for HeHCN and $V_{\mathrm{HF}}(R)$ represents the repulsive interaction of Born-Meyer type and may be given by

$$V_{\mathrm{HF}}(R) = A \exp(-bR - cR^2) \quad (3)$$

which may also be written as $V_{\mathrm{HF}}(R) = exp(a - bR - cR^2)$ for pairs of atoms involving He. A (or a), b, and c are parameters obtained from a least-squares fit to restricted open-shell Hartree−Fock (RHF) ab initio calculations as discussed below. The second term, $V_{\mathrm{dc}}(R)$, of the right-hand side of eq 2 is the dynamical correlation energy, and it has been modeled[36] semiempirically by the damped dispersion series expansion

$$V_{\mathrm{dc}}(R) = -\sum_{n=6,8,10} \chi_n(R) C_n / R^n \quad (4)$$

where C_n are the dispersion energy coefficients and χ_n are dispersion damping functions defined as[26]

$$\chi_n(R) = [1 - \exp(-A_n x - B_n x^2)]^n \quad (5)$$

where $x = R/\rho$ is a reduced coordinate and ρ a scaling parameter given by[26,32]

$$\rho = 5.5 + 1.25 R_0 \quad (6)$$

with R_0 being defined the LeRoy distance[37] for onset of the undamped R^{-n} expansion. In turn, for two interacting atoms A and B, one has

$$R_0 = 2(\langle r_{\mathrm{A}}^2 \rangle^{1/2} + \langle r_{\mathrm{B}}^2 \rangle^{1/2}) \quad (7)$$

with $\langle r_{\mathrm{A}}^2 \rangle$ and $\langle r_{\mathrm{B}}^2 \rangle$ being the expectation values of the squared radii for the outermost electrons in atoms A and B, respectively; A_n and B_n are given in terms of universal parameters α_0, α_1, β_0, and β_1 as $A_n = \alpha_0 n^{-\alpha_1}$ and $B_n = \beta_0 \exp(-\beta_1 n)$, respectively, where $\alpha_0 = 16.36606$, $\alpha_1 = 0.70172$, $\beta_0 = 17.19338$, and $\beta_1 = 0.09574$. The values of other parameters are given in Table 1.

2.2. ES Potential Energy Surface. An accurate global energy-switching strategy for the potential energy surface of polyatomic systems was presented by one of us.[38,39] Accordingly, the ES potential energy surface for HeHCN can be written as follows:

$$V_{\mathrm{ES}} = f(\Delta E) V_1(\mathbf{R}) + [1 - f(\Delta E)] V_2(\mathbf{R}') \quad (8)$$

TABLE 1: Parameters of DMBE Potential Energy Surface

						dispersion coefficients		
	$\lambda_{He\beta}$	A	b	c	R_0	C_6	C_8	C_{10}
HeH	0.2047	0.327 043	1.361 48	0.045 654 1	5.6409	2.823	41.83	871.30
HeC	6.2907	0.622 917	1.115 93	0.103 813	6.1224	7.14	116.29	2481.36
HeN	1.3951	2.283 06	1.601 63	0.047 225 5	5.4688	5.90	80.80	1448.91

where $V_1(\mathbf{R})$ is the DMBE potential energy surface $V(\mathbf{R})$ of eq 1 and $V_2(\mathbf{R}')$ is the function $V(R,\theta)$ used by Atkins and Hutson[5] added to the global HCN DMBE potential energy surface.[35] Thus, $V_2(\mathbf{R}')$ is a 5D-dimensional potential energy surface as implied by the prime, which causes no problem when obtaining the final potential energy surface in eq 8, because this is obviously a function valid over the full-dimensional configuration space $\mathbf{R}$. In turn, ΔE is defined by

$$\Delta E = E - E_0 \tag{9}$$

and gives the displacement from some reference energy (in the energy space defined by V_2), whereas $f(\Delta E)$ is a switching function that approaches 0 for large negative energy displacements ($\Delta E \rightarrow -\infty$) and +1 for large positive ones ($\Delta E \rightarrow +\infty$). V_{ES} changes smoothly from $V_1(\mathbf{R})$ to $V_2(\mathbf{R}')$ as the energy varies across E_0, which is accomplished by the switching function $f(\Delta E)$. This should be system specific, but following previous work,[38,39] we may write it as follows:

$$f(\Delta E) = \frac{1}{2}[1 + \tanh(\gamma \Delta E)] \tag{10}$$

With this form of f, eq 8 assumes the form

$$V_{ES} = f(\Delta E)V_1(\mathbf{R}) + f(-\Delta E)V_2(\mathbf{R}) \tag{11}$$

An optimum value of γ was so determined by trial and error for a selected reference energy, from the requirement that V_{ES} should give a good description of the rovibrational spectra of HeHCN and not invite spurious topographical features at other regions of configuration space. Note that V_{ES} would become 5D only when $\Delta E \rightarrow -\infty$. Of course, although $f(\Delta E)$ is calibrated to attain very small values at specific regions, it never becomes zero because both merged potential energy surfaces are bounded below.

2.3. Bound States and Microwave Transitions. Rovibrational levels of HeHCN were obtained through solutions of the bound-state Schrödinger equation as a set of coupled differential equations,[40] using a Hamiltonian of the form

$$H = -\frac{\hbar^2}{2\mu} R^{-1} \frac{d^2}{dR^2} R + H_{int} + V(R, \theta) \tag{12}$$

where H_{int} is the internal Hamiltonian of the pseudodiatomic (i.e., HCN), and $V(R,\theta)$ is the interaction potential in Jacobi coordinates, including the centrifugal interaction. The former is obtained by subtracting the potential of HCN from $V_{ES}(\mathbf{R})$, with the internal coordinates of HCN frozen at the specific values chosen for the calculation. The BOUND program[41] was used to solve eq 12, using a space-fixed basis set including all HCN rotor functions up to $j = 14$. The rotational constant of HCN and the reduced mass of the complex were 1.478 221 834 cm^{-1} and 3.486 027 184 m_u respectively. The grid for the R coordinate was determined by $R_{min} = 2$ Å and $R_{max} = 10$ Å with a step size of 0.05 Å. The frequencies of microwave transitions were then obtained from the differences of corresponding energy levels by using the usual Bohr rules.

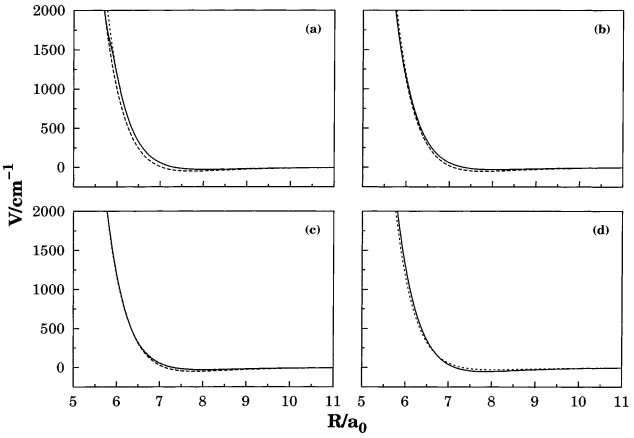

Figure 1. Comparison of plots of He···HCN (v_1, 0, v_3) potential energy surface by DMBE, ES, and 1E8 methods in vibrational states: (a) (0, 0, 0), (b) (1, 0, 2), (c) (2, 0, 3), and (d) (1, 0, 5).

3. Results and Discussion

To obtain the DMBE potential energy surface, the two-body and three-body interaction energy terms for HCN were, following spin-spatial Wigner−Witmer rules, treated as in ref 34. For diatomics HeH, HeC, and HeN, the potentials V_{HF} were calculated ab initio for ground states $^2\Sigma^+$, $^3\Sigma^-$, and $^4\Sigma^-$, respectively, using the augmented correlation consistent quadruple-ζ (VQZ) basis sets[42−45] in a RHF scheme. Calculations were done using the MOLPRO package.[46] The calculated ab initio potentials were used to fit the parameters A (or a), b, and c of eq 3 as described above. Table 1 gives the values of these parameters. The asymptotic standard errors are generally within 6% for bond distances $4 < R/a_0 < 10$.

The parameter $\lambda_{He\beta}$ was determined from consideration of obtaining a correct behavior at dissociation limits as well as a smooth potential well for He···HCN interaction. One way to ensure it could be to minimize the *rmsd* of this model potential from reference ab initio energies.[7] We have chosen it in a different way. It is considered that the component $V_{He\beta}$ of DMBE potential $V(\mathbf{R})$ of eq 1 is mainly coming from the HF energy, and $V_{HF}(R)$ and its coefficient $\lambda_{He\beta}$ merely rescales it. So it should have more or less the same value for He···HCN as for Ar···HCN interaction, considering the otherwise similarities of Rg−HCN chemistry. Assuming the transferability of such parameters, we have taken them identical to the optimum values found in the ArHCN case. Its value are collected in Table 1.

Such a behavior of DMBE potential, as noted above, is even more important from the standpoint of the ES potential energy surface. In the latter case, the parameters E_0 and γ of eqs 9 and 10 were obtained by trial and error done from the requirement that the ES function should reproduce the lowest microwave transition. This also ensures a smooth rather than a sharp switch from DMBE potential energy surface to a reference ab initio surface as shown in Figure 1a. We have obtained a value of 1709.5 cm^{-1} for the reference energy E_0 and 0.003 cm^{-1} for γ.

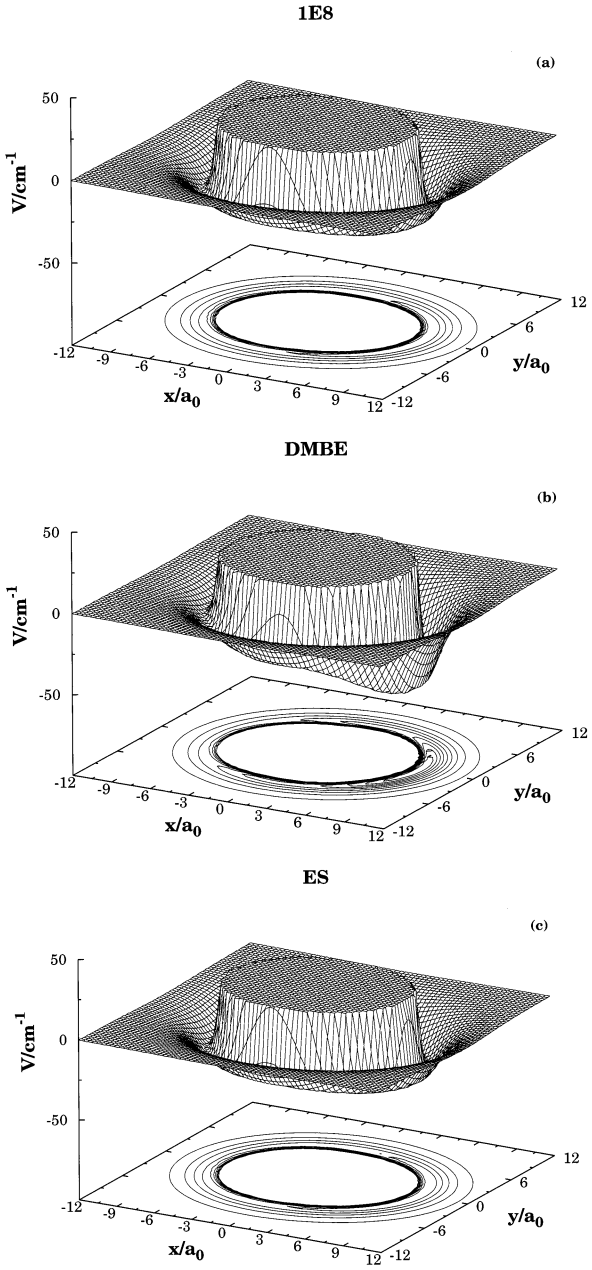

Figure 2. Perspective view/contour plot of HeHCN potential energy surface for an He atom moving around an HCN molecule frozen at its linear equilibrium geometry (a) 1E8, (b) DMBE, and (c) ES.

3.1. Potential Well. A perspective view/contour plot of the 1E8, DMBE, and ES potential energy surfaces with $\theta = 0$ may be seen in Figure 2a−c. The plot obtained by the 1E8 parametrizaton of Atkins and Hutson[5] has also been included for comparison. All potential energy surfaces exhibit a linear global minimum. The DMBE potential energy surface shows the deepest well (-49.95 cm^{-1}) at $R = 4.09$ Å. The greater depth of the well is expected because of the nonconsideration of some three-body and four-body terms in the expansion. Nevertheless, the DMBE potential energy surface shows a satisfactory asymptotic behavior, which makes it useful for the study of reaction dynamics and kinetics. The ES potential well is -29.47 cm^{-1} found at $R = 4.27$ Å (these values coincide with those of 1E8), in agreement with the well obtained by Atkins and Hutson.[5]

An equal well depth obtained by both the methods, ES and 1E8, confirms our assumption of transferability of the scaling parameter, $\lambda_{x\beta}$, where x = Ar or He [cf. eq 2]. It also closely agrees with the well of -29.90 cm^{-1} at $R = 4.22$ Å reported by Toczylowski et al.,[15] using the CCSD (T) scheme. Both Atkins et al.,[5] with 2E8 parametrization and Toczylowski et al.[15] report a local minimum also. It is found at somewhat smaller separation of about 3.6 Å, with a small nonlinear equilibrium geometry. However, we do not find it, either by DMBE or ES methods, because this is based on 1E8. The ab initio calculations of Drucker et al.[4] done at MP4 level, upon which Atkins et al.[5] base their calculations, do not also exhibit such a minimum. Drucker et al.,[4] however, reported a global minimum about 4 cm^{-1} higher at $R = 4.27$ Å.

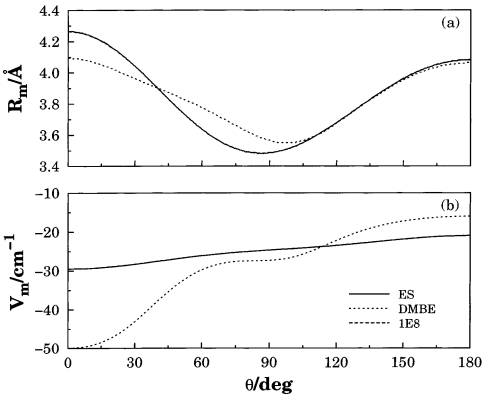

Figure 3. Variation of position and depth of potential well of HeHCN for $0 < \theta < \pi$: (a) $R_m(\theta)$ and (b) $V_m(\theta)$.

With heavier members of the Rg−HCN series, for example, the Ar−HCN, a deeper well with a linear global minimum of about -85.0 and -173.1 cm^{-1}, respectively, at about 4.63 Å was found by the ES and DMBE methods,[7,8] respectively. Toczylowski et al.[15] found it at 147.0 cm^{-1} at 4.5 Å.

The functions $R_m(\theta)$ and $V_m(\theta)$ giving the position of energy minimum and well depth plotted against θ for $0 < \theta < \pi$ are compared in Figure 3. Each of the functions obtained from the ES surface runs coincidently with that obtained from 1E8 surface. The functions obtained from DMBE surface have some differences. Here, the well is deeper and obtained at smaller separation, $R_m(\theta)$, for reasons explained above. The function $R_m(\theta)$ has a minimum at around $\theta = 85°$ for ES or 1E8 and around $\theta = 100°$ for DMBE potential energy surfaces. It is around this minimum that DMBE function $V_m(\theta)$ has a point of inflection. Although $R_m(\theta)$ obtained by the DMBE method runs more or less parallel to the one obtained for the ES or the 1E8 functions, $V_m(\theta)$ obtained by the DMBE method has an interesting oscillatory dependence on θ. Such an oscillatory behavior is not unexpected as observed by Atkins and Hutson[5] in the case of the 2E8 parametrization.

3.1.1. Effect of Bond Stretching. With stretch of the CN or CH bonds, both the polarizability and short-range repulsion may be expected to increase, lending greater depth to the wells and pushing the repulsive wall away. In fact, the ES potential energy surface shows slightly deeper wells with increasing stretch, with its repulsive wall getting closer to the (unstretched) 1E8 repusive wall, vide Figure 1a−c. With still greater stretch, it goes even beyond 1E8, as may be seen in Figure 1d. For this investigation, we have used both the systematic increase of CN or CH stretch and the expectation values of the bond lengths for higher vibrational states (v_1, v_2, and v_3), where the subscripts 1 and 3 refer to the normal modes for symmetric and asymmetric stretching of HCN and 2 refers to its bending normal mode (the bending quantum number v_2 has been constrained to the

TABLE 2: Effect of CN and CH Stretching on the He···HCN Potential Well

	⟨*r*⟩[a]		⟨*R*⟩		*r*(H−C−N)		ES		DMBE	
(v_1, v_2, v_3)	scaled[c]	unscaled	scaled[c]	unscaled	scaled	unscaled	R_m	ϵ[b]	R_m	ϵ
0 0 0	2.1920	2.2020	3.1961	3.2143	4.2080	4.2308	8.06	−29.4669	7.74	−49.9460
1 0 0	2.2058	2.2159	3.2061	3.2244	4.2244	4.2474	8.06	−29.4670	7.74	−49.9461
0 0 1	2.1942	2.2042	3.2519	3.2705	4.2648	4.2881	8.06	−29.4682	7.74	−49.9500
2 0 0	2.2199	2.2300	3.2161	3.2345	4.2409	4.2640	8.06	−29.4673	7.75	−49.9450
1 0 2	2.2099	2.2200	3.3210	3.3400	4.3412	4.3649	8.06	−29.4811	7.79	−51.1006
0 0 3	2.2090	2.2191	3.3889	3.4082	4.4084	4.4324	8.04	−30.4813	7.81	−51.6613
6 0 0	2.2781	2.2885	3.2562	3.2748	4.3079	4.3313	8.06	−29.5662	7.79	−49.9224
2 0 3	2.2253	2.2355	3.3962	3.4156	4.4235	4.4476	8.03	−31.0126	7.82	−51.6176
1 0 5	2.2053	2.2154	3.4967	3.5167	4.5148	4.5394	7.86	−52.2952	7.86	−52.3249

[a] All distances *r*, *R*, and R_m (giving the position of energy minimum) are in Bohr (a_0). [b] ϵ is the well depth in cm^{-1}. [c] See the text for a definition of scaled distances.

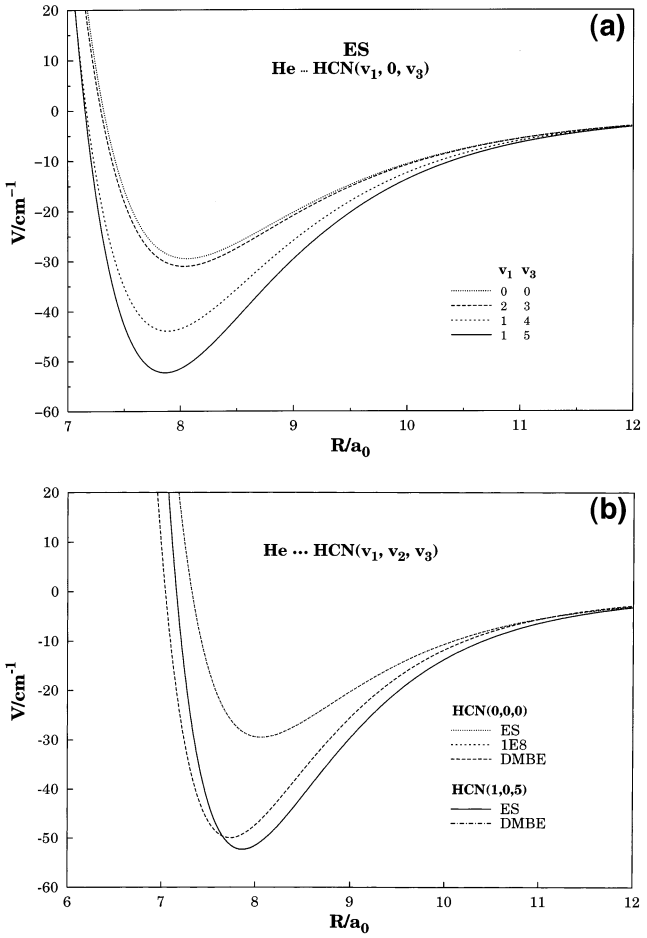

Figure 4. Comparison of potential wells of different states of HeHCN. Panel (a): (i) (1, 0, 5)/ES, (ii) (1, 0, 5)/DMBE, (iii) (0, 0, 0)/ES, (iv) (0, 0, 0)/1E8, and (v) (0, 0, 0)/DMBE. Panel (b): (i) (0, 0, 0)/1E8, (ii) (2, 0, 3)/ES, (iii) (1, 0, 4)/ES, and (iv) (1, 0, 5)/ES.

value zero to make the molecule remain linear). In both cases, we obtain identical results as discussed below.

The well is usually deeper, though to a small extent, in higher states corresponding to greater stretch, as may be seen in Figure 4. For a particular stretch, the repulsive DMBE wall completely coincides with the 1E8 ab initio surface in the repulsive region, [see Figure 1c]. Thus, Figure 4a compares representative ES wells for different stretches in states (2,0,3), (1,0,4), and (1,0,5) of HCN against that of the 1E8 (0,0,0) state [ES and 1E8 wells coincide for the (0,0,0) state)], whereas Figure 4b compares DMBE, ES, and 1E8 wells for the HCN vibrational state (0,0,0) on one hand and compares DMBE wells for the (0,0,0) and (1,0,5) states on the other [the ES and DMBE wells of state (1,0,5) coincide]. The ES well for the most stretched state (1,0,5) is seen to be the deepest solely on account of the larger contribution of DMBE to the ES formulation. The wells obtained by the DMBE and ES methods for representative states have been collected in Table 2, along with effective linear H−C−N distance obtained as sum of expectation values of CN and CH bond lengths scaled by a factor so as to have these bond lengths in the (0,0,0) state equal to their equilibrium values. For example, the expectation values of *r*(CN) and *r*(OH), where O is center of mass of CN, are 2.2020 a_0 and 3.2143 a_0 in state (0,0,0). They were multiplied by scaling factors 0.995 46 and 0.994 33 to obtain their equilibrium values 2.1920 and 3.1961 a_0, respectively. The same scaling factors were used to scale *r*(CN) and *r*(OH) bond lengths/distances of all other states. Both the DMBE and the ES wells obtained with inward or outward stretch may be seen to go deeper similarly. We have studied bound states with CN and CH bonds stretched according to different vibrational modes. Table 3 presents values calculated for some of these stretches of the two frequencies for ground-state transitions $J = 1 \leftarrow 0$ and $J = 2 \leftarrow 1$ that were observed at 15.9 and 31.3 GHz by Drucker et al.[4] They are discussed later.

3.2. Topographical Features. Though topographically the ES and 1E8 potential energy surfaces look similar [Figure 2, parts c and a], there is an important difference; the ES has the correct short and long-range behavior as it entails the salient features of both the DMBE and 1E8 surfaces. As shown in Figure 1a, the ES scheme warrants a smooth transition from the high energy regions to low energy regions, where the van der Waals potential V_2 (here, 1E8) is valid and offers (see below) a good representation of bound states. For high energy regions, the DMBE provides better promise for kinetics studies.[7] The ES potential energy surface can therefore be expected to offer both the bound-state and dynamical properties of the system. In fact, our dynamics studies are in progress.

3.3. Bound States and Microwave Transitions. The bound state levels obtained from the ES energy surface are shown in Figure 5. The Figure also shows, for comparison, rovibrational levels as obtained from the 1E8 surface. Clearly, the two sets of levels are very close together and are indistinguishable within the scale of Figure 5. However, the ES levels are slightly lower compared to 1E8 levels in general. The frequencies of the corresponding microwave transitions are given in Table 4. They may be seen to be in good agreement with experiment. The 1E8 frequencies are also given in Table 4 for comparison.

The first two transitions observed at 15.9 and 31.3 GHz by Drucker et al.[4] are well brought out by our bound-state calculations using the ES potential energy surface. The calculations also bring out successfully the transitions observed at 101.4, 105.8, and 4.6 GHz. However, the one observed by

TABLE 3: Microwave Frequencies of States of Different Stretching Modes

assignment v_1, v_2, v_3 parity	rotational constant[a] B_e, cm^{-1}	frequency/MHz v_1 for j, L, J (0, 1, 1) ← (0, 0, 0) observed[b]	ES	v_2 for j, L, J (0, 2, 2) ← (0, 1, 1) observed	ES
0 0 0 e	1.478 221 834[b]	15893.6108	15 893.6108	31 325.2443	31 325.3070
0 0 1 e	1.468 15		15 882.9424		31 299.3279
1 0 0 e	1.467 80		15 882.5751		31 298.4279
2 0 0 e	1.457 08		15 870.9654		31 270.1407
1 0 2 e	1.448 05		15 860.9619		31 245.7727
0 0 3 e	1.446 03		15 858.6883		31 240.2460
2 0 3 e	1.427 11		15 837.0345		31 187.4400

[a] From ref 47. [b] From ref 4.

TABLE 4: Comparison of ES and 1E8 Microwave Frequencies (ν) in MHz

assignments of frequency (j, L, J)	ν^a (observed)	ν^b (calculated) 1E8	ν^c (calculated) ES
(0,1,1) ← (0,0,0)	15 893.6108	15 893.6125	15 893.6108
(0,2,2) ← (0,1,1)	31 325.2443		31 325.3070
$24D_j$	461.9773	461.9825	461.9145
(1,1,2) ← (0,1,1)	101 432.0813	101 432.1050	101 421.9844
(1,2,3) ← (0,2,2)	105 795.3110	105 795.0313	105 782.1624
(1,2,3) ← (1,2,2)	4604.2000	4604.4200	4598.5816
(1,0,1) ← (0,0,0)		98 603.1200	98 594.9390
(1,1,1) ← (0,1,1)		97 892.1300	97 885.3896
(0,3,3) ← (0,2,2)		45 767.1200	45 769.6546
(1,3,3) ← (0,3,3)		106 633.3200	106 626.1382

[a] From ref 4. [b] From ref 5. [c] This work.

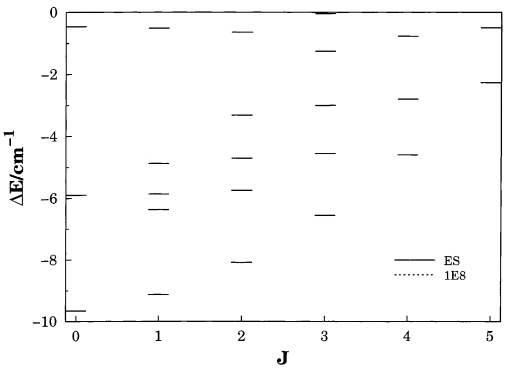

Figure 5. Comparison of rovibrational levels of HeHCN: (a) ES and (b) 1E8.

Drucker et al.[4] at 101.2 GHz could not be obtained both by our ES or the 1E8 calculations of Atkins and Hutson.[5] However, this transition might be associated with some stretching mode. The transition $(j, L, J) = (1, 1, 2) \leftarrow (0, 1, 1)$ observed at 101.4 GHz may get perturbed under stretch, leading to lowering of its frequency to 101.2 GHz. Such a lowering has been observed in our calculations (see Table 3). The ES potential energy surface thus seems to hold some promise to explain rovibrational levels and associated microwave transitions.

Although the DMBE levels are lower, the values of the corresponding frequencies agree fairly closely with those of experiment, ES and 1E8. They are, however, lower by about 1 GHz. It turns out that DMBE is closer to the 1A8 type of potential form proposed by Atkins and Hutson,[5] as the two predict such spectroscopic properties more similarly.

Coming to the next heavier member of Rg−HCN series, the frequency of the lowest $J = 1 \leftarrow 0$ rovibrational transition was calculated to be 5.52 cm^{-1} by the ES method[8] for Ar−HCN. This may be compared to the corresponding frequency of HeHCN which is about 0.53 cm^{-1} or about 15893 MHz (vide Table 4).

It may be noted that bound states of different rovibrational levels corresponding to different stretching of CN and CH bonds may form an interesting spectroscopic study of HeHCN. Such a study can further help in understanding if different rovibrational transitions can occur in the same vibrational state as observed experimentally by Drucker et al.[4] Some initial results are given in Table 3. It may be seen that the frequency of transition generally decreases with greater stretch associated with higher energy states.

4. Concluding Remarks

The global 6D potential energy surfaces for HeHCN have been calculated by the DMBE and ES methods. They correctly behave at all dissociation limits. However, the ES surface reproduces the properties of the van der Waals molecule better. The quality of the surface has been examined by its ability to reproduce the frequencies of rovibrational transitions. Suitability of the surface to study varied spectroscopic features such as the effect of bond stretching on rovibrational levels and subsequent changes of frequencies of the corresponding microwave transitions has been investigated. The initial results as reported here are encouraging. Our study on dynamics of the reaction He + HCN → He + H + CN is currently in progress. The ES potential energy surface reported in this paper is, to our knowledge, the only existing one which is capable of reproducing both the bound states and kinetics of the HeHCN molecule, although some important shortcoming may still be remaining.

Acknowledgment. W.H.A. thanks Dr. S. P. J. Rodrigues and P.J.B.S. Caridade, Departamento de Química, Universidade de Coimbra, Portugal, for computational assistance, and expresses his indebtedness to Professor N. Sathyamurthy of the Indian Institute of Technology, Kanpur, India, for continuous encouragements. This work has the support of Fundação para a Ciência e Tecnologia, Portugal.

References and Notes

(1) Green, S.; Thaddeus, P. *Astrophys. J.* **1974**, *104*, 653.
(2) Clary, D. C.; Dateo, C. E.; Stoecklin, T. *J. Chem. Phys.* **1990**, *93*, 7666.
(3) Gutowsky, H. S.; Keen, J. D.; Germann, T. C.; Emilsson, T. *J. Chem. Phys.* **1993**, *98*, 6801.
(4) Drucker, S.; Tao, F.-H.; Klemperer, W. *J. Phys. Chem.* **1995**, *99*, 2646.
(5) Atkins, K. M.; Hutson, J. M. *J. Chem. Phys.* **1996**, *105*, 440.
(6) Umera, K.; Hara, A.; Tanaka, K. *J. Chem. Phys.* **1996**, *104*, 9747.
(7) Rodrigues, S. P. J.; Varandas, A. J. C. *J. Phys. Chem. A* **1998**, *102*, 6266.
(8) Varandas, A. J. C.; Rodrigues, S. P. J.; Gomes, P. A. J. *Chem. Phys. Lett.* **1998**, *297*, 458.
(9) Cybulski, S. M.; Couvillion, J.; Klos, J.; Chalasinski, G. *J. Chem. Phys.* **1999**, *110*, 1416.
(10) Tanaka, K.; Bailleux, S.; Mizoguchi, A.; Harda, K.; Baba, T.; Ogawa, I.; Shirasaka, M. *J. Chem. Phys.* **2000**, *113*, 1524.

(11) Toczylowski, R. R.; Cybulski, S. M. *J. Chem. Phys.* **2000**, *112*, 4604.
(12) Lee, H.-S.; McCoy, A. B.; Toczylowski, R. R.; Cybulski, S. M. *J. Chem. Phys.* **2000**, *113*, 5736.
(13) Cybulski, S. M.; Toczylowski, R. R.; Lee, H.-S.; McCoy, A. B. *J. Chem. Phys.* **2000**, *113*, 9549.
(14) Murdachaew, G.; Misquitta, A. J.; Bukowski, R.; Szalewicz, K. *J. Chem. Phys.* **2001**, *114*, 764.
(15) Toczylowski, R. R.; Doloresco, F.; Cybulski, S. M. *J. Chem. Phys.* **2001**, *114*, 851.
(16) Cambell, E. J.; Buxton, L.; Legon, A. C. *J. Chem. Phys.* **1983**, *78*, 3483.
(17) Leopold, K. R.; Fraser, G. T.; Lin, F. J.; Nelson, D. D., Jr.; Klemperer, W. *J. Chem. Phys.* **1984**, *81*, 4922.
(18) Klots, T. D.; Dykstra, C. E.; Gutowsky, H. S. *J. Chem. Phys.* **1989**, *90*, 30.
(19) Mladenović, M.; Bacic, Z. *J. Chem. Phys.* **1991**, *94*, 4988.
(20) Yaron, D.; Klemperer, W. *J. Chem. Phys.* **1991**, *95*, 1907.
(21) Cooksy, A. L.; Drucker, S.; Faeder, J.; Gottlieb, C. A.; Klemperer, W. *J. Chem. Phys.* **1991**, *95*, 3017.
(22) Tao, F.; Drucker, S.; Klemperer, W. *J. Chem. Phys.* **1995**, *102*, 7289.
(23) Bowman, J. M.; Padmavathi, D. A. *Mol. Phys.* **1996**, *88*, 21.
(24) Bumgarner, R. E.; Blake, G. A. *Chem. Phys. Lett.* **1989**, *161*, 308.
(25) Fraser, G. T.; Pine, A. S. *J. Chem. Phys.* **1989**, *91*, 3319.
(26) Varandas, A. J. C. *Adv. Chem. Phys.* **1988**, *74*, 255.
(27) Varandas, A. J. C. *Chem. Phys. Lett.* **1992**, *194*, 333.
(28) Varandas, A. J. C. In *Dynamical Processes in Molecular Physics*; Delgado-Barrio, G., Ed.; IOP Publishing: Bristol, 1993; p 3.
(29) Bruehl, M.; Schatz, G. C. *J. Phys. Chem.* **1988**, *92*, 7223.
(30) Hippler, H.; Schranz, H. W.; Troe, J. *J. Phys. Chem.* **1986**, *90*, 6158.
(31) Varandas, A. J. C.; Silva, J. D. *J. Chem. Soc., Faraday Trans. 2* **1986**, *82*, 593.
(32) Varandas, A. J. C.; Silva, J. D. *J. Chem. Soc., Faraday Trans.* **1992**, *88*, 941.
(33) Murrell, J. N.; Carter, S.; Farantos, S. C.; Huxley, P.; Varandas, A. J. C. *Molecular Potential Energy Functions*; Wiley: Chichester, U.K., 1984.
(34) Varandas, A. J. C. In *Reaction and Molecular Dynamics*; Laganá, A., Riganelli, A., Eds.; Springer: Berlin, 2000; Vol. 75 of *Lecture Notes in Chemistry*, p 33.
(35) Varandas, A. J. C.; Rodrigues, S. P. J. *J. Chem. Phys.* **1997**, *106*, 9647.
(36) Varandas, A. J. C. *Mol. Phys.* **1987**, *60*, 527.
(37) Le Roy, R. J. *Spec. Period. Rep. Chem. Soc. Mol. Spectrosc.* **1973**, *1*, 113.
(38) Varandas, A. J. C. *J. Chem. Phys.* **1996**, *105*, 3524.
(39) Varandas, A. J. C. *J. Chem. Phys.* **1997**, *107*, 867.
(40) Hutson, J. M. *Comput. Phys. Comm.* **1994**, *84*, 1.
(41) Hutson, J. M. BOUND computer code, version 5; distributed by Collaborative Computational Project No. 6 of the Science and Engineering Research Council, U.K., 1993.
(42) Dunning, T. H., Jr. *J. Chem. Phys.* **1989**, *90*, 1007.
(43) Kendall, R. A.; Dunning, T. H., Jr.; Harrison, R. J. *J. Chem. Phys.* **1992**, *96*, 6796.
(44) Woon, D. E.; Dunning, T. H., Jr. *J. Chem. Phys.* **1994**, *100*, 2975.
(45) Wilson, A. A.; Woon, D. E.; Peterson, K. A.; Dunning, T. H., Jr. *J. Chem. Phys.* **1999**, *110*, 7667.
(46) Werner, H.-J.; Knowles, P. J. MOLPRO is a package of ab initio programs written by H.-J. Werner, P. J. Knowles, with contributions from J. Almlöf, R. D. Amos, M. J. O. Deegan, S. T. Elbert, C. Hampel, W. Meyer, K. A. Peterson, R. Pitzer, A. J. Stone, P. R. Taylor, R. Lindh, 1998.
(47) Carter, S.; Mills, I. M.; Handy, N. C. *J. Chem. Phys.* **1993**, *99*, 4379.